Simulation studies of multi-line line-of-sight tunable-diode-laser absorption spectroscopy performance in measuring temperature probability distribution function*

Zhang Guang-Le(张光乐), Liu Jian-Guo(刘建国)†, Kan Rui-Feng(阚瑞峰), and Xu Zhen-Yu(许振宇)

Key Laboratory of Environmental Optics & Technology, Anhui Institute of Optics and Fine Mechanics, Chinese Academy of Sciences, Hefei 230031, *China*

(Received 29 March 2014; revised manuscript received 30 May 2014; published online 10 October 2014)

Line-of-sight tunable-diode-laser absorption spectroscopy (LOS-TDLAS) with multiple absorption lines is introduced for non-uniform temperature measurement. Temperature binning method combined with Gauss–Seidel iteration method is used to measure temperature probability distribution function (PDF) along the line-of-sight (LOS). Through 100 simulated measurements, the variation of measurement accuracy is investigated with the number of absorption lines, the number of temperature bins and the magnitude of temperature non-uniformity. A field model with 2-T temperature distribution and 15 well-selected absorption lines are used for the simulation study. The Gauss–Seidel iteration method is discussed for its reliability. The investigation result about the variation of measurement accuracy with the number of temperature bins is different from the previous research results.

Keywords: TDLAS, temperature non-uniformity, Gauss–Seidel iteration method, simulation

PACS: 42.62.Fi, 02.70.–c **DOI:** 10.1088/1674-1056/23/12/124207

1. Introduction

As a robust, nonintrusive and commercially available technology with fast response time and high sensitivity, line-of-sight tunable-diode-laser absorption spectroscopy (LOS-TDLAS) is widely used in combustion diagnostics for measuring temperature and product concentration. Traditionally, it is employed to monitor the uniform or nearly uniform flow fields and obtain the average temperature or species concentration along the laser path.[1–5] However, significant non-uniformities in temperature and species concentration exist in many practical flow fields. They are typically caused by flow boundary layers, heat transfer between surfaces, flow mixing, inhomogeneous combustion zones, buoyancy, and phase change. LOS-TDLAS has been previously extended to measure the non-uniform flow fields. Ouyang and Varghese proposed an energy-temperature curve method to correct the thermal boundary layer effects.[6] Wang *et al.* offered a way to reduce effects of the non-uniformities.[7] Palaghita and Seitzman correlated a pattern factor with the path-averaged temperatures inferred from different line pairs.[8]

In this paper we explain an attractive strategy for temperature non-uniformity measurement, i.e., LOS-TDLAS with multiple absorption lines, which Sanders *et al.* well demonstrated by using O_2 absorption lines,[9] and so did Liu *et al.* with H_2O lines[10] and other predecessors.[11–13] Liu *et al.* also obtained the temperature PDF solutions with temperature binning strategy. In the present paper, the temperature binning strategy combined with Gauss–Seidel iteration method is further proposed, explained and discussed for obtaining the temperature PDF solutions. And the variation of its accuracy is investigated with the number of absorption lines, the number of temperature bins and the magnitude of temperature non-uniformity, which is instructive to obtain better results in the actual measurement of temperature PDF.

2. Theoretical principles

2.1. Lambert–Beer law

In the measurement, an incident laser beam is collimated into the target field and the transmitted laser is received by a detector. According to the Lambert–Beer law, the laser intensity along a differential path length of dx attenuates, following

$$\frac{-\mathrm{d}I_\nu}{I_\nu} = P \cdot \sum_{l=1}^{K} X_{\mathrm{abs},i}(x) \cdot \sum_{i=1}^{N_l} S_{i,l}(T(x)) \times \Phi_{i,l}(\nu - \nu_{0,i}) \cdot \mathrm{d}x, \quad (1)$$

where I_ν is the laser intensity, P (in unit atm, 1 atm = 1.01325×10^5 Pa) is the total pressure, $T(x)$ is the local temperature (in unit K), $X_{\mathrm{abs},i}(x)$ is the mole fraction of species l, K is the total number of species, N_l is the total number of transitions of the species l, $S_{i,l}$ (in unit $\mathrm{cm}^{-2}\cdot\mathrm{atm}^{-1}$) and $\Phi_{i,l}$ (in unit cm) are the line strength and line shape of a particular transition i of the species l respectively. And the line strength of a particular transition i, which is temperature-dependent,

*Project supported by the National Natural Science Foundation of China (Grant No. 61108034) and the Young Scientists Fund of the National Natural Science Foundation of China (Grant No. 61205151).

†Corresponding author. E-mail: jgliu@aiofm.ac.cn

© 2014 Chinese Physical Society and IOP Publishing Ltd

can be described in terms of the known line strength at a reference temperature T_0:

$$\begin{aligned} & S_i(T) \\ &= S_i(T_0)\frac{Q(T_0)}{Q(T)}\left(\frac{T_0}{T}\right)\exp\left[-\frac{hcE_i''}{k}\left(\frac{1}{T}-\frac{1}{T_0}\right)\right] \\ &\quad\times\left[1-\exp\left(\frac{-hc\nu_{0,i}}{kT}\right)\right]\left[1-\exp\left(\frac{-hc\nu_{0,i}}{kT_0}\right)\right]^{-1}, \end{aligned} \tag{2}$$

where h (in unit J·s) is the Planck constant, c (in unit cm/s) is the speed of light, k (in unit J/K) is Boltzmann constant, $Q(T)$ is the partition function of the absorbing molecule, T_0 is the reference temperature (usually 296 K), $\nu_{0,i}$ (in unit cm^{-1}) and E_i'' (in unit cm^{-1}) are the line-center frequency and lower state energy of the transition i respectively.

The absorbance α_ν for a particular transition i of species l is defined as

$$\begin{aligned} \alpha_{\nu,i,l} &\equiv -\ln(\frac{I_\mathrm{t}}{I_0})_\nu \\ &= P\cdot\int_0^L X_{\mathrm{abs},l}(x)\cdot S_{i,l}(T(x))\cdot\Phi_{i,l}(\nu-\nu_{0,i})\cdot\mathrm{d}x, \end{aligned} \tag{3}$$

where I_0 is the incident laser intensity and I_t is the transmitted laser intensity. Because the line shape function $\Phi_{i,l}(\nu-\nu_{0,i})$ is normalized as $\int_{-\infty}^{+\infty}\Phi_{i,l}(\nu-\nu_{0,i})\cdot\mathrm{d}\nu\equiv 1$, the integrated absorbance $A_{i,l}$ (in unit cm^{-1}) can be inferred from Eq. (3) as

$$\begin{aligned} A_{i,l} &= \int_{-\infty}^{\infty}\alpha_\nu\,\mathrm{d}\nu \\ &= P\cdot\int_0^L X_{\mathrm{abs},l}(x)\cdot S_{i,l}(T(x))\cdot\mathrm{d}x. \end{aligned} \tag{4}$$

When the gas is distributed uniformly or nearly uniformly along the path length, equation (4) can be presented as

$$A_{i,l} = P\cdot X_{\mathrm{abs},l}\cdot\int_0^L S_{i,l}(T(x))\cdot\mathrm{d}x. \tag{5}$$

2.2. Temperature PDF solving

H_2O vapor is selected as the target gas with a nearly uniform distribution along the optical path. Decompose the whole path into n sections, each with a nearly uniform temperature of T_j, an absorber mole fraction of X_abs, and path length of L_j. Then equation (5) can be rewritten as

$$A_i = P\cdot X_\mathrm{abs}\cdot\sum_{j=1}^{n}[S_i(T_j)\cdot L_j]. \tag{6}$$

When m absorption lines are selected in the measurement, a linear equation set is formed as follows:

$$\begin{bmatrix} S_1(T_1) & S_1(T_2) & \cdots & S_1(T_n) \\ S_2(T_1) & S_2(T_2) & \cdots & S_2(T_n) \\ \vdots & \vdots & \vdots & \vdots \\ \vdots & \vdots & \vdots & \vdots \\ S_m(T_1) & S_m(T_2) & \cdots & S_m(T_n) \end{bmatrix}\cdot\begin{bmatrix} P\cdot X_\mathrm{abs}\cdot L_1 \\ P\cdot X_\mathrm{abs}\cdot L_2 \\ \vdots \\ P\cdot X_\mathrm{abs}\cdot L_n \end{bmatrix} = \begin{bmatrix} A_1 \\ A_2 \\ \vdots \\ \vdots \\ A_m \end{bmatrix}. \tag{7}$$

There are many methods to solve the above linear equation set. We adopt the Gauss–Seidel iteration method in the following computation, before doing so we should verify the convergence of Gauss–Seidel iterative matrix. The iterative matrix is derived from the coefficient matrix which should be transformed into a square matrix by premultiplying the transposition of coefficient matrix ($\boldsymbol{S}$) on both sides of equal sign of Eq. (7) as shown below

$$\boldsymbol{S}'\cdot\boldsymbol{S}\cdot(P\cdot\boldsymbol{X}_\mathrm{abs}\cdot\boldsymbol{L}) = \boldsymbol{S}'\cdot\boldsymbol{A}. \tag{8}$$

Take $\boldsymbol{S}''\cdot\boldsymbol{S}$ as a new coefficient matrix which can be converted into the iterative matrix after several conversions, while taking $\boldsymbol{S}''\cdot\boldsymbol{A}$ as a new constant matrix. Thus equations (7) and (8) are equivalent and have the same solutions, i.e., $P\cdot\boldsymbol{X}_\mathrm{abs}\cdot\boldsymbol{L}$.

Divide the solution by $P\cdot\boldsymbol{X}_\mathrm{abs}$, then we will obtain the path length L_j $(j=1,2,\ldots,n)$ which is divided by the total path length L to obtain the fraction of path length (F_j) for each bin as expressed below

$$F_j = \frac{L_j}{L},\ \ (j=1,2,\ldots,n). \tag{9}$$

Equation (9) is the final solution, temperature PDF, which, in this paper, is what we are interested in.

3. Methods

The whole simulation process includes preparations and simulation via MATLAB software.

First, select optimal absorption lines for the simulation. According to the selection criteria,[14–16] 15 lines (shown in Table 1) of H_2O within candidate wavelengths in a range of 1.3 μm–1.5 μm are chosen from the HITRAN 2008 database and reconstructed into 5 subsets, each subset containing a different number of absorption lines, i.e. $m=3,5,7,11,15$ (shown in Table 2).

Second, define a specific field for simulation, which is characterized with water vapor concentration (X_{H_2O}), total pressure (P), total path length (L), and a temperature distribution $(T(x))$. $X_{H_2O}=10\%$; $P=1$ atm; $L=10$ cm. And $T(x)$ is a two-T temperature profile (Fig. 1) described with three parameters, i.e., T_h, T_c, and L_c, among which T_h is the temperature of hot region, T_h the temperature of relatively cold region with length L_c. $L_\mathrm{c}=3$ cm, and $T_\mathrm{h}=2000$ K. The difference between T_h and T_c describes the magnitude of temperature non-uniformity (ΔT) of the field. According to different values of ΔT, i.e., 200 K, 400 K, 600 K, 800 K, and 1000 K, the true values of T_c are 1800 K, 1600 K, 1400 K, 1200 K, and

1000 K respectively. For different numbers of unknowns to be solved, the total path length L is divided into n sections, $n = 3$, 5, 7, 9 and n also means the number of temperature bins. The information mentioned above can be summarized into Table 3.

Table 1. 15 absorption lines well selected for simulation.

Line number	ν_0/cm^{-1}	S (296 K) cm^{-2}/atm	E''/cm^{-1}
1	6807.8344	1.02×10^{-6}	3319.4478
2	6864.98033	1.39×10^{-5}	2660.9453
3	6919.9475	$2.14E \times 10^{-4}$	2073.5156
4	6945.48522	5.58×10^{-4}	1774.7511
5	6998.80973	2.42×10^{-3}	1255.1667
6	7057.36796	5.40×10^{-3}	888.5987
7	7397.57463	5.08×10^{-2}	704.214
8	7380.01052	9.47×10^{-2}	552.9114
9	7390.13185	8.53×10^{-2}	446.5107
10	7134.98155	6.48×10^{-2}	382.5169
11	7348.40428	2.25×10^{-1}	300.3623
12	7168.43701	2.90×10^{-1}	173.3658
13	7205.24611	2.46×10^{-1}	79.4964
14	7242.37075	2.95×10^{-1}	42.3717
15	7294.12308	4.04×10^{-1}	23.7944

Table 2. Five subsets with different numbers of absorption lines.

Number of lines	Line number
3	1, 8, 13
5	(3 lines) + 3, 6
7	(5 lines) + 10, 12
11	(7 lines) + 2, 4, 5, 14
15	(11 lines) + 7, 9, 11, 15

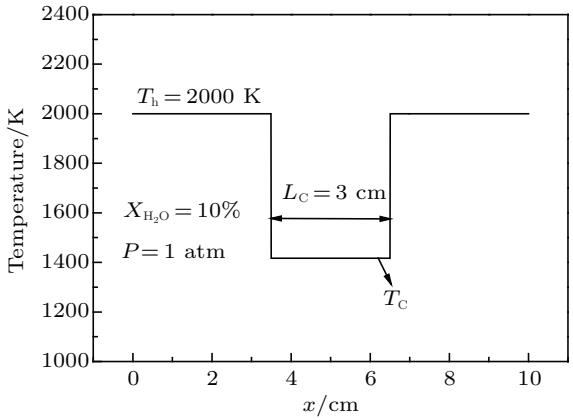


Fig. 1. Field for simulation with two-T temperature profile, with 10% water vapor uniformly distributed and at a pressure of 1 atm.

Table 3. Parameters used in simulations.

	m	ΔT/K	T_c/K	T_h/K	n	L_c/cm	L/cm
I	5 7 11 15	800	1200	2000	5	3	10
II	15	200 400 600 800	1200	1400 1600 1800 2000	5	3	10
III	15	800	1200	2000	3 5 7	3	10

Third, simulate the measurements via MATLAB. At the very beginning, produce a random Gaussian white noise with a standard deviation of 5%. Impose this noise on the true integrated absorbance to simulate the measured data. And then simulate the measurements 100 times to obtain 100 groups of temperature PDF solutions by Gauss–Seidel iteration method. Afterwards calculate root mean square of standard deviation and residual (RMS_STD & RMS_Res.) of every 100 groups of results, to evaluate the accuracy of measurement of temperature PDF. The two parameters mentioned above are defined as follows:

$$\mathrm{RMS_STD} = \sqrt{\frac{\sum_{j=0}^{n} (\mathrm{STD}_j)^2}{n}}, \tag{10}$$

$$\mathrm{RMS_Res.} = \sqrt{\frac{\sum_{j=0}^{n} \left(\overline{F_{\mathrm{measured},j}} - F_{\mathrm{true},j}\right)^2}{n}}, \tag{11}$$

where $F_{\mathrm{true},j}$ is the true value of path length fraction of each bin, $\overline{F_{\mathrm{measured},j}}$ is the averaged fraction of path length of each bin, STD_j is the standard deviation of 100 groups of results for each bin. And the algebra expressions of the latter two parameters are as follows:

$$\mathrm{STD}_j = \sqrt{\frac{\sum_{i=1}^{100} \left|F_{\mathrm{measured}i,j} - \overline{F_{\mathrm{measured}i,j}}\right|^2}{100 - 1}}, \tag{12}$$

$$\overline{F_{\mathrm{measured},j}} = \frac{\sum_{i=1}^{100} F_{\mathrm{measured},i}}{100}. \tag{13}$$

4. Results and discussion

The final results are shown in Figs. 2–4. From Fig. 2(b), we can see an obviously decreasing trend in the STD of temperature PDF solutions obtained with an increasing number of absorption lines. Although the decrease in the residual of PDF solutions is not so obvious, a decreasing trend in it can still be observed. In Fig. 3(b), there is also an obvious decrease in the STD and an unobvious decrease in the residual of solutions obtained with the growing temperature non-uniformity. Figure 4(d) shows that the STD and residual of solutions decrease as the number of temperature bins increases. In other words, we can conclude that the accuracy of simulation measurements improves with increasing the number of absorption lines, the growing temperature non-uniformity, and the increasing temperature bins.

However, the conclusion is quite different from that of the preceding research by Liu who demonstrated that the accuracy of simulation measurements decreases as the number of bins increases.[15] Also, PDF solutions of our own deviate more from the true values than predecessors'. And our STDs of PDF solutions are lower than predecessors'. These differences may derive from the different selected absorption lines and the different methods of simulation measurement. In the predecessors' PDF solutions taken were constrained linear least-square fitting methods and selected were 16 absorption

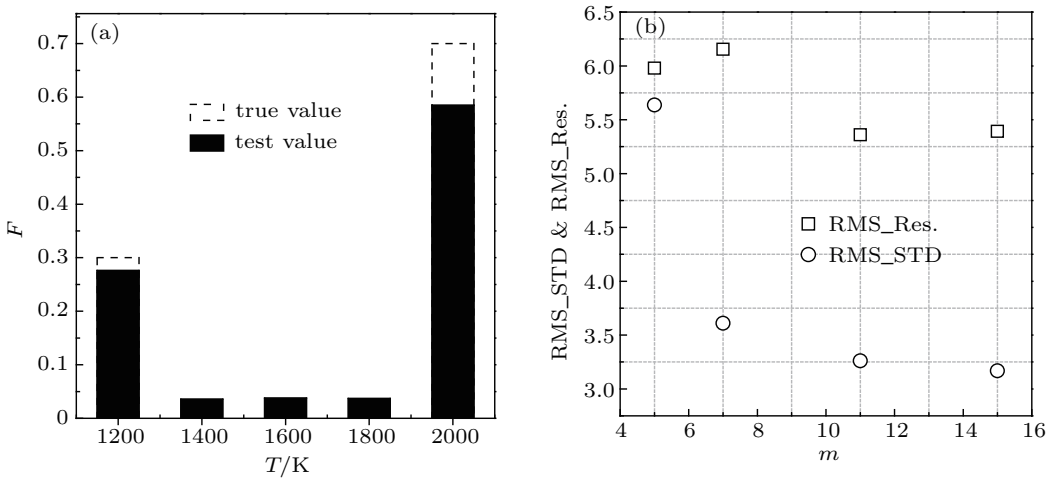


Fig. 2. Simulation results for the field of Fig. 1 ($\Delta T = 800$ K, 5 bins): (a) illustration of the averaged fraction-of-path-length solution solved with 5 absorption lines, (b) the RMSs of STD and residual of the fraction-of-path-length solutions obtained with different numbers of absorption lines.

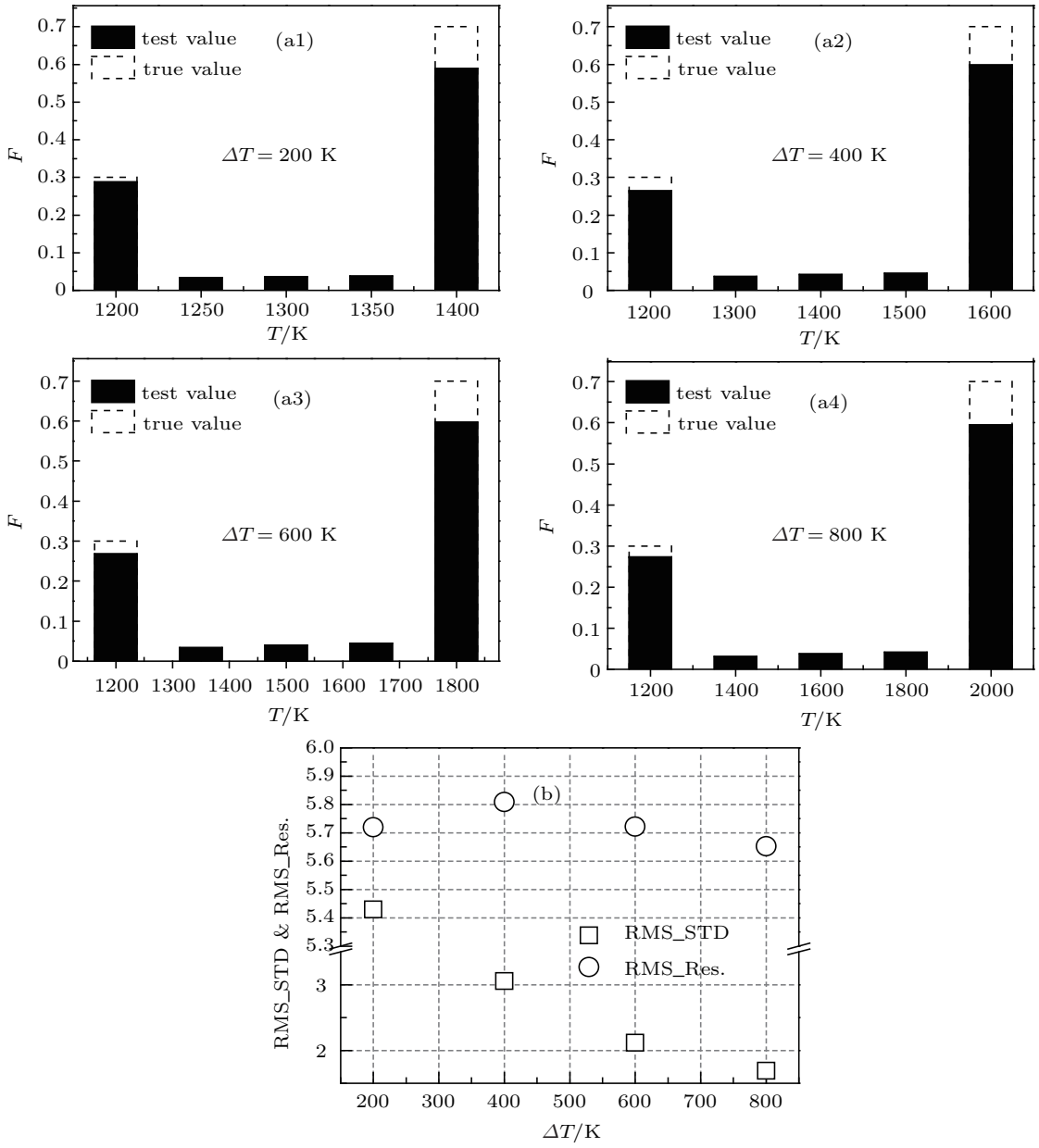


Fig. 3. Influence of temperature non-uniformity magnitude ΔT on the simulation results for the field of Fig. 1 (15 lines and 5 bins): (a1)–(a4) the averaged fraction-of-path-length solutions (F); (b) the RMSs of STD and residual of the fraction-of-path-length solutions for different magnitudes of ΔT.

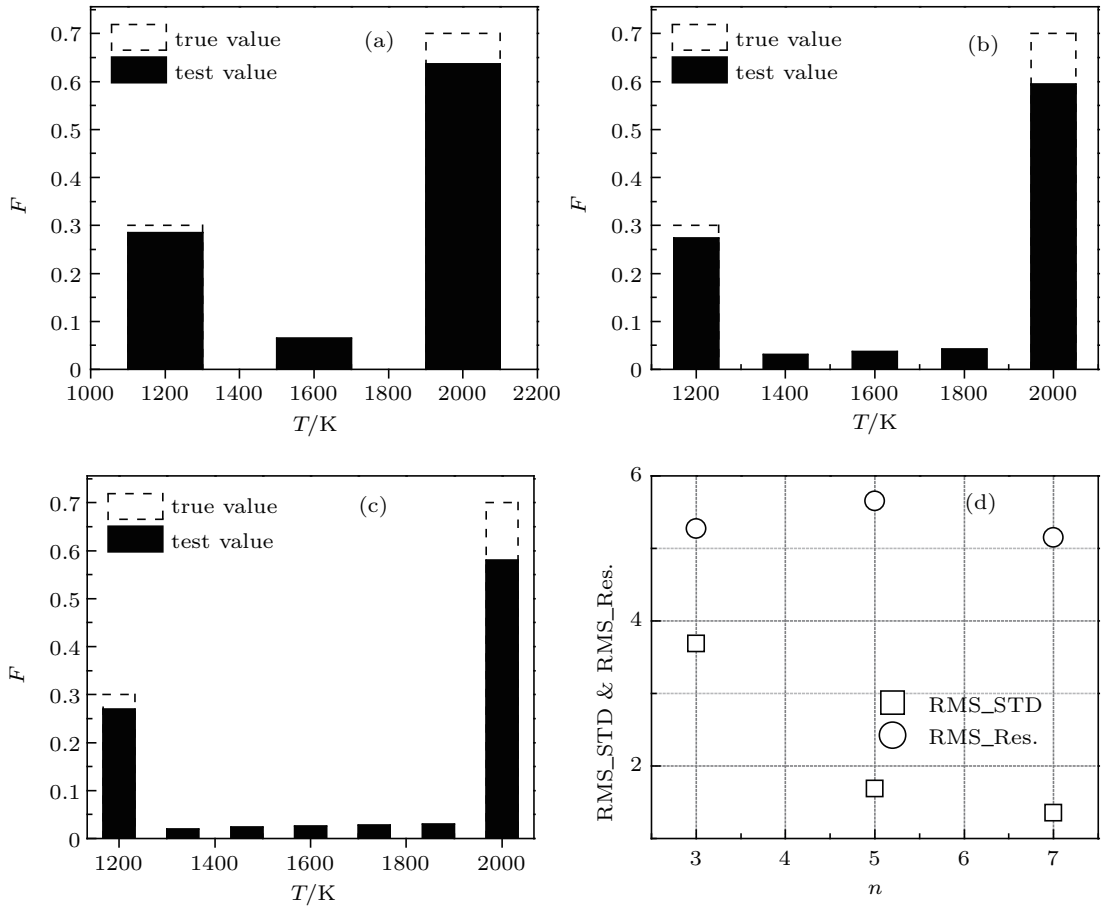


Fig. 4. Influences of number of temperature bins on the simulation results for the field of Fig. 1 (15 lines and $\Delta T = 800$ K), (a)–(c) the averaged fraction-of-path-length solutions (F) for 3 bins, 5 bins, and 7 bins; (d) the RMSs of residual and STD of the fraction-of-path-length solutions for different numbers of bins.

lines with well-spread E'' (79 cm^{-1}–3440 cm^{-1}). In our PDF solutions, we adopt the Gauss–Seidel iteration method with a precision controller of 10^{-3} (the distance between the two sequential iterative solutions), a maximum iteration time of 200, and 15 selected absorption lines spreading over a wide range of E'' (23 cm^{-1}–3320 cm^{-1}).

Considering the above differences shown through the figures, we test the Gauss–Seidel iteration method in several ways. First, we verify the convergence of each iterative matrix once more, and each one used in the simulation is convergent. Second, we test the influence of initial value on the performance of Gauss–Seidel method. We take the products of true value and 100 random figures between 0 and 1 as the initial values. Then we use 100 groups of initial values to test the influence. These tests show that different initial values have little influence on the final iterative results. Third, we test the influences of maximum iteration times and the precision controller, and obtain the same conclusion as the above. Fourth, we compare Gauss–Seidel iteration method with the matrix left division method and linear least square fitting method provided by MATLAB. The result from the iteration method is much better than those from other two methods. Finally, from the study in this paper we draw a conclusion that the method used in the computational simulation is reliable.

It should be noted that all these results are based on the well-selected absorption lines.

5. Conclusion

Through simulating the measurements of temperature probability distribution function of a specific field, we have the conclusion that with the well-selected absorption lines and the Gauss–Seidel iteration method, the accuracy of results improves as the number of absorption lines increases, the magnitude of temperature non-uniformity increases or the number of temperature bins increases in a proper range. This conclusion can help us considerably to obtain better results in the real experiments.

All these results are based on the well-selected absorption lines. Therefore, the selection of absorption lines also plays a very important role in measuring the temperature non-uniformity.

References

[1] Hanson R K and Falcone P K 1978 *Appl. Opt.* **17** 2477
[2] Webber M E, Wang J and Sanders S T 2000 *P. Combust. Inst.* **28** 407

[3] Liu J T C, Rieker G B and Jeffries J B 2005 *Appl. Opt.* **44** 6701
[4] Cai T D, Jia H, Wang G S, Chen W D and Gao X M 2009 *Sensor Actuat. A: Phys.* **152** 5
[5] Xu Z Y, Liu W Q, Liu J G, He J F, Yao L, Ruan J, Chen J Y, Li H, Yuan S, Geng H and Kan R F 2012 *Acta Phys. Sin.* **61** 234204 (in Chinese)
[6] Ouyang X and Varghese P L 1989 *Appl. Opt.* **28** 3979
[7] Wang J, Maiorov M, Jeffries J B, Garbuzov D Z, Connolly J C and Hanson R K 2000 *Meas. Sci. Technol.* **11** 1576
[8] Palaghita T and Seitzman J M 2005 41*st AIAA/ASME/SAE/ASEE Joint Propulsion Conference and Exhibit*, July10–13, 2005, Tucson, USA, p. 3578
[9] Sanders S T, Wang J, Jeffries J B and Hanson R K 2001 *Appl. Opt.* **40** 4404
[10] Liu X, Jeffries J B and Hanson R K 2007 *AIAA Journal* **45** 411
[11] Yu X, Li F, Chen L H and Zhang X Y 2010 *Acta Mech. Sin.* **26** 147
[12] Liu C, Xu L J and Cao Z 2013 *Appl. Opt.* **52** 4827
[13] Li N, Yan J H, Wang F, Chi Y and Cen K J 2008 *Spectrosc. Spect. Anal.* **28** 17082 (in Chinese)
[14] Zhou X, Jeffries J B and Hanson R K 2005 *Appl. Phys. B* **81** 711
[15] Liu X 2006 "Line-of-sight Absorption of H_2O Vapor: Gas Temperature Sensing in Uniform and Nonuniform Flows" (Ph. D. dissertation) (Stanford: Stanford University)
[16] Zhou X, Liu X, Jeffries J B and Hanson R K 2003 *Meas. Sci. Technol.* **14** 1459